

# Carbon nanotubes as ultra-high quality factor mechanical resonators

A. K. Hüttel<sup>1,\*</sup>, G. A. Steele<sup>1</sup>, B. Witkamp<sup>1</sup>, M. Poot<sup>1</sup>, L. P. Kouwenhoven<sup>1</sup> and H. S. J. van der Zant<sup>1</sup>

<sup>1</sup>*Kawli Institute of NanoScience, Delft University of Technology, PO Box 5046, 2600 GA, Delft, The Netherlands.*

## Abstract

We have observed the transversal vibration mode of suspended carbon nanotubes at millikelvin temperatures by measuring the single-electron tunneling current. The suspended nanotubes are actuated contact-free by the radio frequency electric field of a nearby antenna; the mechanical resonance is detected in the time-averaged current through the nanotube. Sharp, gate-tuneable resonances due to the bending mode of the nanotube are observed, combining resonance frequencies of up to  $\nu_0 = 350$  MHz with quality factors above  $Q = 10^5$ , much higher than previously reported results on suspended carbon nanotube resonators. The measured magnitude and temperature dependence of the Q-factor shows a remarkable agreement with the intrinsic damping predicted for a suspended carbon nanotube. By adjusting the RF power on the antenna, we find that the nanotube resonator can easily be driven into the non-linear regime.

High-quality resonating systems, providing high frequency resolution and long energy storage time, play an important role in many fields of physics. In particular in the field of nanoelectromechanical systems [1, 2], recent research has led to the development of high-frequency top-down fabricated mechanical resonators with high quality factors [3, 4, 5, 6]. However, when miniaturizing mechanical resonators to make them lighter and to increase their resonance frequency [1], the quality factor tends to decrease significantly from surface effects [2]. High Q-values combined with high resonance frequencies are an important prerequisite for applications such as single-atom mass sensing [7, 8, 9] and fundamental studies of the quantum limit of mechanical motion [10]. Single-wall carbon nanotubes present a potentially defect-free nanomechanical system with extraordinary mechanical properties: in particular the high Young's modulus ( $E = 1.2$  TPa) in combination with a very low mass density ( $\rho = 1350$  kg/m<sup>3</sup>) [8, 11, 12, 13]. While these favorable properties should result in quality factors of the order of  $2 \times 10^5$  [14], the observed Q-factors of nanotube resonators both at room temperature [11, 12, 15, 16] and in low temperature experiments [7, 8] have not exceeded  $Q \sim 2000$ .

Here we report on the observation of mechanical resonances of a driven suspended carbon nanotube at low temperatures with quality factors above  $10^5$  and resonance frequencies ranging from 120 MHz to 360 MHz. The resonances are detected with a novel detection scheme which uses the non-linear gate-dependence of the current through the suspended nanotube quantum dot. In addition, we show that the nanotube resonator can easily be tuned to the non-linear regime, and that the operating temperature affects the non-linearity and the quality factor of the resonator.

Suspended carbon nanotube devices are made by growing nanotubes between platinum electrodes over an 800 nm wide pre-defined trench. The device geometry is shown in Figure 1(a). The fabrication method is discussed in detail by Steele *et al.* [17]. There, the device includes three local gates for tuning the confinement: here, however, we apply the same voltage to all three gates, so that they act together as one single gate. Since no device processing takes place after nanotube growth and the entire device is suspended, the nanotubes are highly defect-free and do not suffer from potential irregularities induced by the substrate surface [17, 18]. The fabrication method also offers the advantage that the resonator is not contaminated with resist residues.

After fabrication, the suspended nanotube devices are mounted in a dilution refrigerator with filtered twisted pair cabling attached to source, drain, and gate contacts (see Figure 1(a)). This configuration allows us to apply dc gate and bias voltages to the suspended nanotube, and measure the current flowing through it. To minimize heating, we drive the nanotube resonator with the electric field radiated from a radio frequency (RF) antenna positioned near the sample ( $\sim 2$  cm) instead of connecting high-frequency cables directly to the sample. Measurements are performed at temperatures down to the base temperature of the mixing chamber of the dilution refrigerator,  $T_{MC} \simeq 20$  mK.

---

\*Present address: Institute for Experimental and Applied Physics, University of Regensburg, 93040 Regensburg, Germany

Figure 1(b) shows the Coulomb oscillations of a semiconducting carbon nanotube with a suspended length of 800 nm. A highly regular addition spectrum with clear four-fold degeneracy is visible, characteristic for a defect-free single-wall carbon nanotube [19, 20]. From the magnetic-field dependence of the position of the Coulomb oscillations close to the semiconducting gap [21], we find the radius of the nanotube,  $r$ , to be between 1-1.5 nm. The value of the semiconducting gap  $\approx 0.3$  eV is estimated from the gate range between electron and hole conduction in the device at low temperatures, which is in agreement with this value for  $r$ .

When an ac voltage  $V_{\text{RF}}$  with frequency  $\nu$  is applied to the antenna, we observe a resonant feature at a well-defined frequency in the dc current flowing through the nanotube. Figure 1(c) shows an example of such a measurement at a large radio frequency (RF) voltage, or equivalently a high generator power. A sharp resonant feature is clearly visible at  $\nu = 294$  MHz. Zooming in on this feature at a lower power (Figure 1(d)) reveals a resonance peak with a narrow lineshape. A numerical fit of this data yields a quality factor  $Q = 140670$  (see below for a discussion of the expected lineshape). We have also performed measurements on a second device displaying similar resonant peaks with Q-factors up to 20000; the results on that device are shown in the Suppl. Information.

The resonance observed in parts (c) and (d) of Figure 1 can be attributed to the flexural vibration mode of the suspended nanotube [8, 7, 11, 12]. To verify this, we electrostatically induce tension in the nanotube by applying a dc gate voltage  $V_g$  to the back gate electrode [11, 12]. The dc gate voltage dependence is shown in Figure 2. When decreasing the gate voltage from zero to more and more negative values, the resonance is tuned to higher frequencies by almost a factor of three: from less than  $\nu_0 = 140$  MHz at  $V_g = -1$  V to  $\nu_0 = 355.5$  MHz at  $V_g = -6.5$  V. For the latter resonance frequency, the thermal occupation [10]  $n = 1/2 + [\exp(h\nu_0/k_B T_{MC}) - 1]^{-1}$  would be 1.2 at 20 mK, suggesting that the resonator would be close to its quantum ground state in the absence of the driving fields required for our detection scheme.

We have extracted the resonance peak positions from the data in Figure 2 and plotted them in the inset. The red line shows the gate dependence of the resonance frequency calculated with a continuum model for the fundamental flexural bending mode [22, 12, 23]. The parameters are  $\nu_{\text{bending}} = 132.0$  MHz,  $V_g^* = -2.26$  V, and  $T_0 = 0$ , where  $\nu_{\text{bending}}$  is the resonance frequency in absence of residual tension  $T_0$  and  $V_g^*$  marks the cross over between the weak and strong bending regime. At high gate-voltage the model calculation deviates slightly from the experimental values. This is so far not fully understood and may be related to large static displacements of the nanotube in a complex electrostatic environment [24]. The value  $\nu_{\text{bending}} = 22.4/2\pi L^2 \cdot r \sqrt{E/\rho} = 132.0$  MHz, assuming a tube length  $L = 800$  nm, yields a nanotube radius of 1.6 nm, in good agreement with the band-gap and magnetic field estimates.

Depending on the gate voltage, the resonance either appears as a dip (Figure 3(a)) or as a peak (Figure 3(b)). Dips are found around the maxima of the Coulomb oscillations; away from these maxima peaks are observed. This indicates that the detection of the mechanical modes is due to electrostatic interactions as we will now show. We model the effect of a small change in gate voltage  $\delta V_g$  on the current flowing through the nanotube by a Taylor expansion of  $I(V_g + \delta V_g)$  around  $\delta V_g = 0$ . A crucial point in this expansion is that the second (and third) order term cannot be neglected, since the current flowing through the nanotube is strongly non-linear in the vicinity of the Coulomb oscillations. This is in contrast to the mixing technique [11, 12], where only the linear term in the expansion is needed.

The motion of the nanotube enters the measured current as follows: On resonance, the nanotube position  $u(t) = u_0 \cos(2\pi\nu_0 t)$  oscillates with a finite amplitude  $u_0$ , which periodically modulates the gate capacitance  $C_g$  by an amount  $C_g^{\text{ac}} = (dC_g/du) u_0$ . The current flowing through the nanotube does not just depend on the gate voltage itself; more specifically, it depends on the product of the gate voltage and the gate capacitance - the so-called gate-induced charge [11, 12, 25]. A modulation of the capacitance due to the motion of the nanotube therefore has the same effect on the current as if an effective ac gate voltage  $V_g^{\text{ac,eff}} = V_g C_g^{\text{ac}}/C_g$  were applied to the gate-electrode. The time-dependent current can then be calculated by inserting  $\delta V_g = V_g^{\text{ac,eff}} \cos(2\pi\nu t)$  into the Taylor expansion of  $I(V_g + \delta V_g)$ .

Since the mechanical resonance frequency is much larger than the measurement bandwidth, time-averaged currents are detected in our setup. We find that the time-averaged mechanically induced current equals:

$$\bar{I}(u_0, V_g) = I(V_g) + \frac{u_0^2}{4} \left( \frac{V_g}{C_g} \frac{dC_g}{du} \right)^2 \frac{\partial^2 I}{\partial V_g^2} + \mathcal{O}(u_0^4), \quad (1)$$

where only even powers of  $u_0$  enter the low-frequency current due to averaging. The change in dc current on mechanical resonance  $\Delta I = \bar{I} - I$  is thus proportional to the local curvature  $\partial^2 I/\partial V_g^2$  of the Coulomb

blockade oscillations  $I(V_g)$ .

Using measured Coulomb oscillation traces where no driving signal was applied (black line in Figure 3(c)), we have numerically calculated the behavior of a current time-averaged over  $V_g^{\text{ac,eff}}$ . The result is shown as a red line in Figure 3(c). Figure 3(d) shows the difference  $\Delta I$  between the time-averaged and the static current of Figure 3(c). On top of a Coulomb oscillation, the curvature is negative and the averaged current (red) is smaller than the static current (black), resulting in a dip in the current on resonance, when mechanical motion takes place. On the other hand,  $\Delta I$  is positive on the flanks of the Coulomb oscillations as the curvature is positive there. This can be compared with the traces  $I(\nu)$  shown in Figure 3(a) and (b), and with the measurements of  $\Delta I$  shown in Figure 3(e). Here we plot the amplitude  $\Delta I(\nu_0)$  of the mechanical response in the dc current  $I(\nu)$  for different gate voltages. The gate voltage dependence of the extracted amplitude values in dc current is in good qualitative agreement with the predictions of the model as shown in Figure 3(d).

The model also allows for a quantitative analysis of the peak shape and for an estimate of the displacement amplitude  $u_0$  in the case of resonant driving, by evaluating the change in dc current  $\Delta I$  alone. We first note that  $u_0$  can be described by the response of a damped driven harmonic oscillator [12, 22]. From Eq. 1, we see that  $\Delta I \propto u_0^2$  so that the measured mechanical response (dip or peak) in the current is given by the square of the harmonic oscillator response function (SHO). For the resonance presented in Figure 1(d), we find  $\nu_0 = 293.428$  MHz and  $Q = 140670$ . This Q-value is nearly two orders of magnitude higher than previous reported values of the flexural vibration modes in nanotubes [7, 8, 11, 12]. Such high Q-values make this type of device very suitable for mass detection. From the measured response in Figure 4(e) we estimate (see Suppl. Information) a mass sensitivity of  $7 \text{ yg}/\sqrt{\text{Hz}}$ , i.e., in one second it should be possible to determine if, for example, a He atom has adsorbed onto the nanotube.

The displacement amplitude  $u_0$  in the case of resonant driving is estimated by modelling the capacitance between the nanotube and the back-gate as the capacitance between an infinite wire and an infinite conductive plane [22]. Using a device length of  $L = 800$  nm, a tube radius  $r = 1.5$  nm and a gate distance  $h_0 = 230$  nm, we obtain  $C_g = 7.8$  aF and  $dC_g/du = -5.9$  zF/nm. The calculated capacitance value is consistent with the experimentally determined value of  $C_g = 8.9$  aF as determined from the Coulomb peak spacing. For the resonance in Figure 4(b), with  $\partial^2 I / \partial V_g^2 = 4.43 \mu\text{A}/V^2$  and  $\Delta I(\nu_0) = 1.05$  pA, we estimate the oscillation amplitude of the nanotube to be  $u_0(\nu_0) = 0.25$  nm on resonance. This amplitude is two orders of magnitude larger than that of the thermal fluctuations ( $k_B T / 2 = m(2\pi\nu_0)^2 u_{th}^2 / 2$ ) of the nanotube [1], which is  $\sim 6.5$  pm at 80 mK, and its estimated zero-point motion [10, 26] of 1.9 pm at this gate voltage.

When driving the nanotube resonator with large antenna voltages, we consistently observe hysteretic peak shapes and a strong frequency pulling of the resonance peaks (i.e. the frequency decreases for a larger motion amplitude [27, 28]). Figure 4(a)-(d) show examples of the shape of the resonance peak at  $V_g = -5.16$  V and  $V_{\text{sd}} = 0.35$  mV for four different driving powers. Black lines indicate the sweep direction with increasing frequency; red lines the one with decreasing frequency. At the lowest power, the mechanical resonance peak is not visible in the noise. With increasing driving power the resonance peak first shows a linear response with its characteristic SHO shape (Figure 4(b)). At higher powers hysteresis sets in, which becomes more pronounced with increasing RF power. This bistability is consistent with what is expected for a non-linear mechanical (Duffing) resonator [1, 27].

We have studied the dynamic range [29, 2, 24, 30] in more detail and found that the driving powers where the (linear) peak disappears in the noise and where nonlinearity sets in depend on the temperature. An example of this effect is shown in Figure 4(e)-(h). These panels show that for a fixed gate voltage and driving power, the nanotube resonator response changes from non-linear to linear when the operating temperature is increased from 20 mK to 160 mK. This temperature-dependent behavior hints at a decrease in Q-factor as the temperature is increased.

To study the temperature dependence of the quality factor in more detail, we have determined  $Q$  at different temperatures. For a gate voltage of -5.16 V, three examples of resonance traces are depicted in Figure 5(a)-(c). Note that because the dynamic range is temperature dependent, the RF power is adjusted at every temperature to ensure a linear response. In Figure 5(d), we plot the Q-factor extracted in the linear regime for eight different temperatures in the range  $20 \text{ mK} < T_{MC} < 1$  K. The error margins are estimated from ensembles of responses at the same temperature. The Q-factor changes by a factor four in this temperature range. At the lowest temperatures, the Q-factor reproducibly reaches values above  $10^5$ . These lowest temperature values are close to the intrinsic Q-values calculated with molecular dynamics simulations

on single-walled carbon nanotube oscillators [14]. Interestingly, these calculations predict a  $T^{-0.36}$  power law dependence of the Q-factor with temperature. The red line in Figure 5(d) shows this dependence; the data is consistent with this prediction. This  $T^{-0.36}$  dependence has also been observed at low temperatures in top-down fabricated devices [31, 6]. Note that the Q-values of our nanotube resonator are much higher than the ones following the trend of the volume surface ratio in top-down fabricated devices [2].

In conclusion, using a novel detection mechanism, we have measured the bending mode resonance of suspended carbon nanotubes in the single-electron tunneling regime. Sharp gate-tunable resonances are found with high Q-values ( $Q > 10^5$ ), which can easily be driven into the nonlinear regime by increasing the driving power on the RF antenna. By inducing tension with a gate voltage the frequency can be tuned above 350 MHz, so that the thermal occupation of the resonator approaches 1. Shorter devices should have even higher resonance frequencies corresponding to temperatures higher than the mixing chamber temperature of the dilution refrigerator. These resonators are therefore in their quantum mechanical ground state, which opens up the way to new exciting experiments on the quantum aspects of mechanical motion.

**Acknowledgement.** The authors thank Yaroslav Blanter and Giorgi Labadze for discussions and Raymond Schouten for experimental help. This research was carried out with financial support from the Dutch Foundation for Fundamental Research on Matter (FOM), The Netherlands Organisation for Scientific Research (NWO), NanoNed, and the Japan Science and Technology Agency International Cooperative Research Project (JST-ICORP).

**Supporting Information Available:** Estimation of the mass sensitivity and measurements on a second device. This material is available free of charge via the Internet at <http://pubs.acs.org>.

## References

- [1] Andrew N. Cleland. *Foundations of Nanomechanics*. Springer, 1 edition, August 2004.
- [2] K. L. Ekinci and M. L. Roukes. Nanoelectromechanical systems. *Rev. Sci. Instrum.*, 76(6):061101, 2005.
- [3] A. Naik, O. Buu, M. D. LaHaye, A. D. Armour, A. A. Clerk, M. P. Blencowe, and K. C. Schwab. Cooling a nanomechanical resonator with quantum back-action. *Nature*, 443(7108):193–196, 2006.
- [4] N. E. Flowers-Jacobs, D. R. Schmidt, and K. W. Lehnert. Intrinsic noise properties of atomic point contact displacement detectors. *Phys. Rev. Lett.*, 98:096804, 2007.
- [5] X. L. Feng, C. J. White, A. Hajimiri, and M. L. Roukes. A self-sustaining ultrahigh-frequency nanoelectromechanical oscillator. *Nature Nanotech.*, 3:342 – 346, 2008.
- [6] Guiti Zolfagharkhani, Alexei Gaidarzhy, Seung-Bo Shim, Robert L. Badzey, and Pritiraj Mohanty. Quantum friction in nanomechanical oscillators at millikelvin temperatures. *Phys. Rev. B*, 72(22):224101, 2005.
- [7] B. Lassagne, D. Garcia-Sanchez, A. Aguasca, and A. Bachtold. Ultrasensitive mass sensing with a nanotube electromechanical resonator. *Nano Lett.*, 8(11):3735–3738, 2008.
- [8] Hsin-Ying Chiu, Peter Hung, Henk W. Ch. Postma, and Marc Bockrath. Atomic-scale mass sensing using carbon nanotube resonators. *Nano Lett.*, 8(12):4342–4346, 2008.
- [9] K. Jensen, Kwanpyo Kim, and A. Zettl. An atomic-resolution nanomechanical mass sensor. *Nat. Nano.*, 3(9):533–537, 2008.
- [10] K. C. Schwab and M. L. Roukes. Putting mechanics into quantum mechanics. *Phys. Today*, page 36, 2005.
- [11] V. Sazonova, Y. Yaish, H. Üstünel, D. Roundy, T. A. Arias, and P. L. McEuen. A tunable carbon nanotube electromechanical oscillator. *Nature*, 431:284, 2004.
- [12] B. Witkamp, M. Poot, and H.S.J. van der Zant. The bending-mode vibration of a suspended nanotube resonator. *Nano Lett.*, 6:2904, 2006.

- [13] B. Witkamp, M. Poot, H. Pathangi, A. K. Hüttel, and H. S. J. van der Zant. Self-detecting gate-tunable nanotube paddle resonators. *Appl. Phys. Lett.*, 93(11):111909, 2008.
- [14] H. Jiang, M.-F. Yu, B. Liu, and Y. Huang. Intrinsic energy loss mechanisms in a cantilevered carbon nanotube beam oscillator. *Phys. Rev. Lett.*, 93(18):185501, Oct 2004.
- [15] K. Jensen, J. Weldon, H. Garcia, and A. Zettl. Nanotube radio. *Nano Lett.*, 7(11):3508–3511, 2007.
- [16] Anders Eriksson, SangWook Lee, Abdelrahim A. Sourab, Andreas Isacsson, Risto Kaunisto, Jari M. Kinaret, and Eleanor E. B. Campbell. Direct transmission detection of tunable mechanical resonance in an individual carbon nanofiber relay. *Nano Letters*, 8(4):1224–1228, 2008.
- [17] G. A. Steele, G. Götz, and L. P. Kouwenhoven. Tunable few-electron double quantum dots and klein tunnelling in ultraclean carbon nanotubes. *Nature Nanotechnology*, 2009. advance online publication, 6 April 2009 (doi:10.1038/nnano.2009.71).
- [18] Jien Cao, Qian Wang, and Hongjie Dai. Electron transport in very clean, as-grown suspended carbon nanotubes. *Nat. Mater.*, 4(10):745–749, October 2005.
- [19] Yuval Oreg, Krzysztof Byczuk, and Bertrand I. Halperin. Spin configurations of a carbon nanotube in a nonuniform external potential. *Phys. Rev. Lett.*, 85(2):365–368, Jul 2000.
- [20] Wenjie Liang, Marc Bockrath, and Hongkun Park. Shell filling and exchange coupling in metallic single-walled carbon nanotubes. *Phys. Rev. Lett.*, 88(12):126801, Mar 2002.
- [21] E. D. Minot, Yuval Yaish, Vera Sazonova, and Paul L. McEuen. Determination of electron orbital magnetic moments in carbon nanotubes. *Nature*, 428(6982):536–539, Apr 2004.
- [22] M. Poot, B. Witkamp, M. A. Otte, and H. S. J. van der Zant. Modelling suspended carbon nanotube resonators. *Physica Status Solidi (b)*, 244:4252, 2007.
- [23] An extended continuum model that includes ac tension effects on the gate-tuning of the resonance, will be published elsewhere.
- [24] I. Kozinsky, Ch. I. Bargatin, and M. L. Roukes. *Applied Physics Letters*, 88(25):253101, 2006.
- [25] Leo P. Kouwenhoven, Charles M. Marcus, Paul L. McEuen, Seigo Tarucha, Robert M. Westervelt, and Ned S. Wingreen. *Electron transport in quantum dots*. NATO ASI conference proceedings. Kluwer, 1997. edited by L. L. Sohn and L. P. Kouwenhoven and G. Schön.
- [26] M. D. LaHaye, O. Buu, B. Camarota, and K. C. Schwab. Approaching the quantum limit of a nanomechanical resonator. *Science*, 304(5667):74–77, 2004.
- [27] Ron Lifshitz and M. C. Cross. *Reviews of Nonlinear Dynamics and Complexity: Volume 1 (Annual Reviews of Nonlinear Dynamics and Complexity)*, chapter 1. Wiley-VCH, June 2008.
- [28] M. C. Cross, A. Zumdick, Ron Lifshitz, and J. L. Rogers. Synchronization by nonlinear frequency pulling. *Physical Review Letters*, 93(22):224101, 2004.
- [29] H. W. Ch. Postma, I. Kozinsky, A. Husain, and M. L. Roukes. Dynamic range of nanotube- and nanowire-based electromechanical systems. *Appl. Phys. Lett.*, 86(22):223105, 2005.
- [30] The lower boundary of the dynamic range is the power at which the resonance is no longer visible in the noise. The current noise in our experiments is caused by fluctuations in the electrostatic environment of the nanotube and not by to the thermal motion of the nanotube.
- [31] Seung Bo Shim, June Sang Chun, Seok Won Kang, Sung Wan Cho, Sung Woon Cho, Yun Daniel Park, Pritiraj Mohanty, Nam Kim, and Jinhee Kim. Micromechanical resonators fabricated from lattice-matched and etch-selective GaAs/InGaP/GaAs heterostructures. *Appl. Phys. Lett.*, 91(13):133505, 2007.

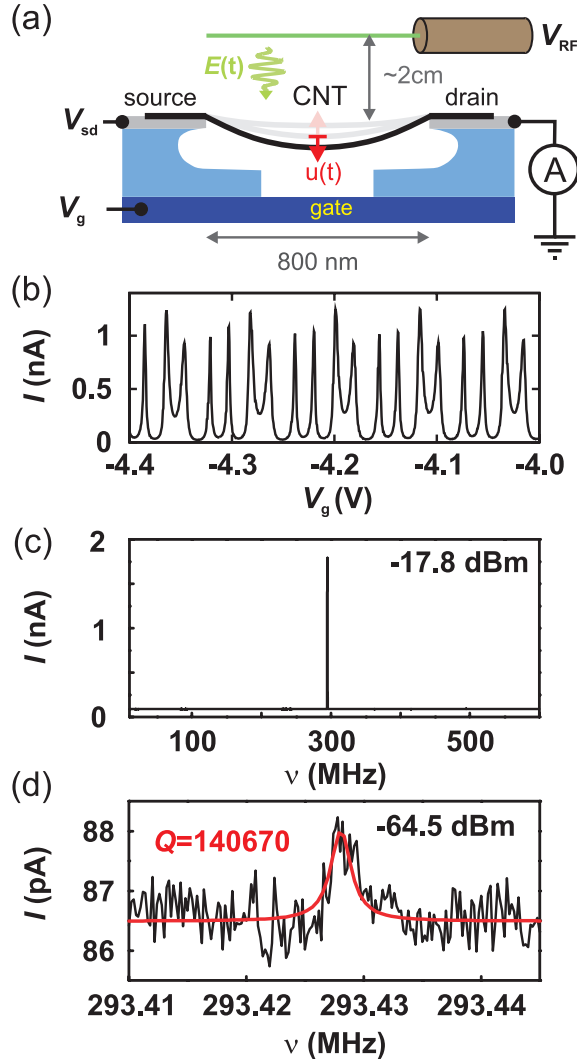


Figure 1: (a) Schematic drawing of the chip geometry, antenna, and measurement electronics. The nanotube acts as a doubly clamped beam resonator, driven by an electric field  $E(t)$ . The displacement of the nanotube is  $u(t)$ . (b) Example trace of the dc current at  $V_{sd} = 50 \mu\text{V}$  as a function of gate voltage, demonstrating the regularity of the Coulomb peaks. It shows the four-fold degeneracy typical for clean single-wall carbon nanotubes. (c) When the frequency  $\nu$  of an RF signal on the antenna is swept with fixed  $V_g$  and  $V_{sd}$ , a resonant peak emerges in  $I(\nu)$ . An example of such a resonance is shown for a driving power of  $-17.8 \text{ dBm}$  at a temperature of 20 mK. (d) Zoom of the resonance of (c) at low power ( $-64.5 \text{ dBm}$ ). The red line is a fit of a squared damped driven harmonic oscillator response to the resonance peak. For both (c) and (d)  $V_g = -5.16 \text{ V}$  and  $V_{sd} = 0.35 \text{ mV}$ .

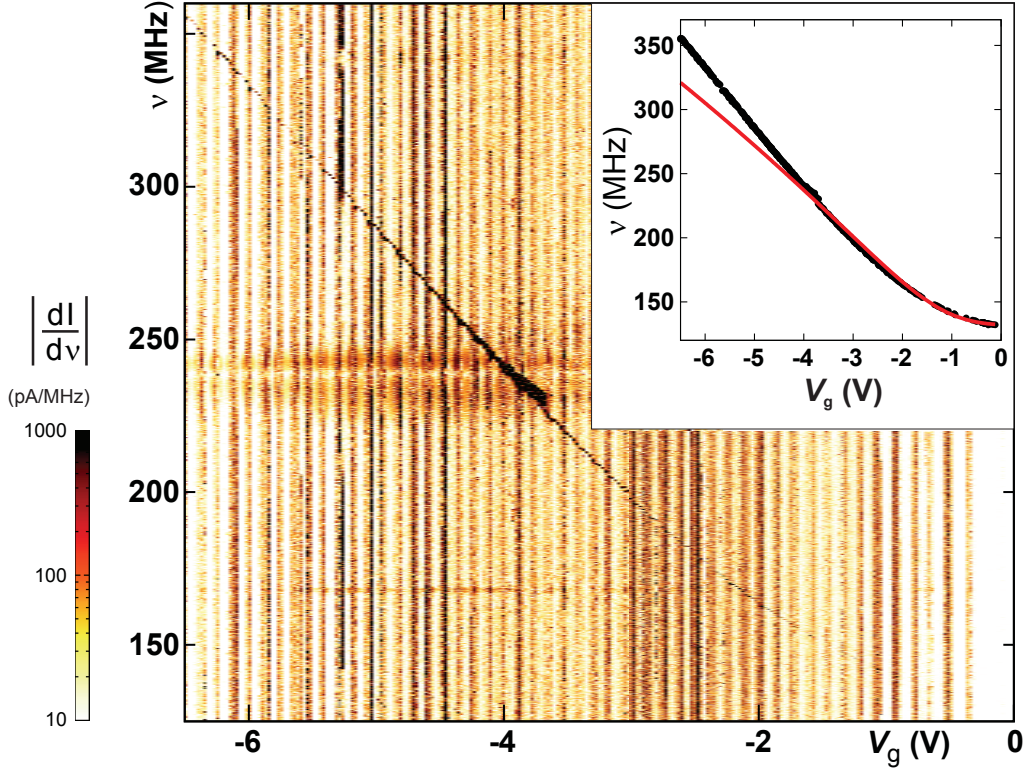


Figure 2:  $|dI/dv|$  as a function of frequency  $\nu$  of the ac voltage on the antenna and the dc gate voltage  $V_g$  on the back-gate electrode. Horizontal stripes are caused by electrical (cable) resonances [11, 12]; the narrow vertical stripe pattern is related to the Coulomb blockade oscillations. In addition, a gate-dependent resonant feature is clearly visible. Inset: Comparison of the extracted resonance frequency to the continuum model for the bending mode with  $\nu_{\text{bending}} = 132.0$  MHz,  $V_g^* = 2.26$  V,  $T_0 = 0$ , and a shift of  $0.775$  V in gate voltage to account for an offset in the charge neutrality point of the nanotube from  $V_g = 0$  V and the band gap region [12, 22]. The parameters are discussed in the text. An apparent shift of the mechanical resonance frequency at  $\nu_0 \simeq 230$  MHz is caused by an electrical (cable) transmission resonance, leading to a strong increase in transmitted RF power and distorted peak shapes.

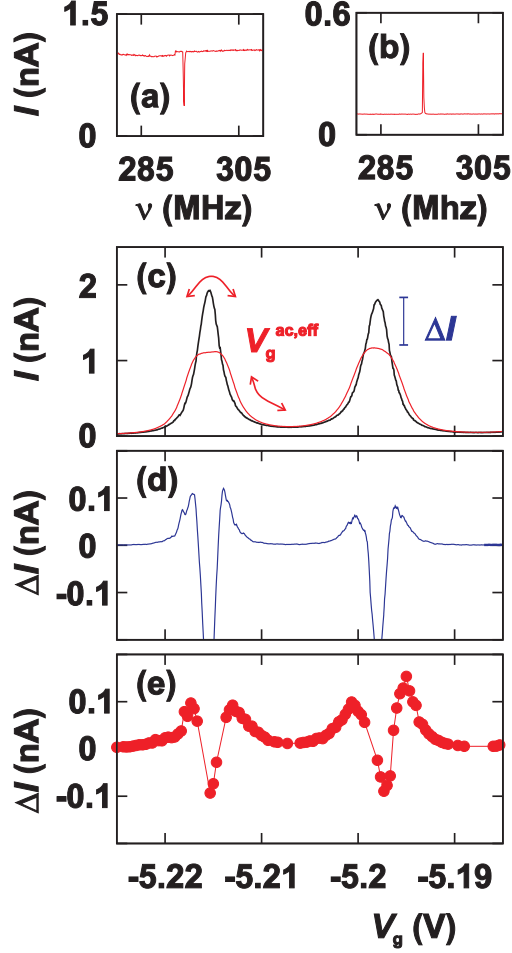


Figure 3: Averaging model for the current at resonance. (a), (b) Measured frequency sweeps demonstrating the sign change of the resonance amplitude depending on the gate voltage (RF power  $-13$  dBm,  $V_{sd} = 0.1$  mV,  $V_g = -5.17$  V (a) and  $V_g = -5.16$  V (b)). (c) The black line shows the measured dc current as function of gate voltage  $I(V_g)$  for  $V_{sd} = 0.1$  mV (no RF). The red line, shows the effect of an (effective) ac gate voltage on the dc current. This average current (Eq. (1)) is calculated using the measured data and  $V_g^{ac,eff} = 2$  mV. (d) Predicted resonance signal amplitude  $\Delta I$  calculated by subtracting the dc current from the current averaged over an effective gate voltage  $V_g^{ac,eff} = 1$  mV. For a small  $V_g^{ac,eff}$ , the signal is proportional to the second derivative  $\partial^2 I / \partial V_g^2$  of the black trace shown in (c), as expressed in Eq. (1). At the top of the Coulomb peak,  $\Delta I$  is negative, whereas on the flanks of the Coulomb peak, it is positive. Note that in (c) a larger value of  $V_g^{ac,eff}$  was used to exaggerate the difference between the black and red curves for illustrative purposes. (e) The measured resonance peak amplitudes obtained from  $I(\nu)$  traces similar to Figure 1(d), for  $V_{sd} = 0.1$  mV and a RF power of  $-48$  dBm.

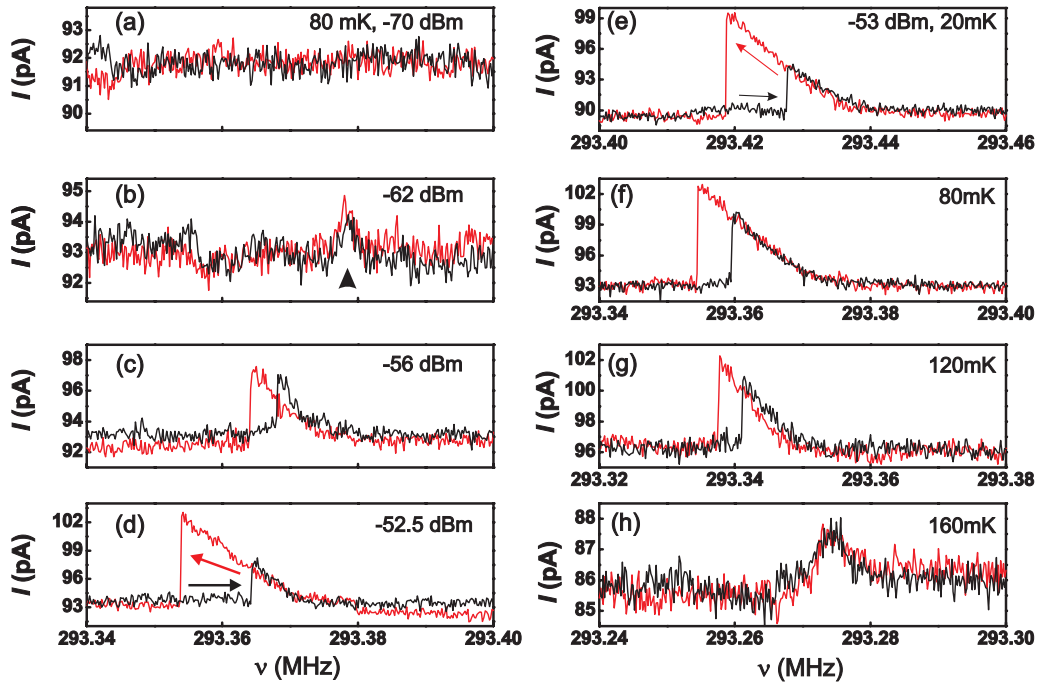


Figure 4: Evolution of the resonance peak with increasing driving power (a-d) and temperature (e-h). Black (red) traces are upward (downward) frequency sweeps. (a) At low powers, the peak is not visible. (b) Upon increasing power, a resonance peak with  $Q=128627$  appears. (c,d) As the power is increased further, the lineshape of the resonance takes on a non-linear oscillator form, with a long high frequency tail and a sharp edge at lower frequencies. It also exhibits hysteresis between the upward and downward sweep that increases with driving power, characteristic of a non-linear oscillator. The traces (a-d) are taken at 80 mK. (e-h) Forward (black) and reverse (red) frequency sweeps at a fixed driving power as a function of temperature. At low temperatures, the peak shape is non-linear and strongly hysteretic. At the same power, but higher temperature, the amount of hysteresis decreases significantly. At a temperature of 160 mK, hysteresis and asymmetry are no longer apparent; at the same time, the signal amplitude (and with it also signal to noise ratio) is decreased, suggesting a decrease in the Q-factor with increasing temperature. The working point of traces (a-h) is at  $V_g = -5.16$  V and  $V_{sd} = 0.35$  mV.

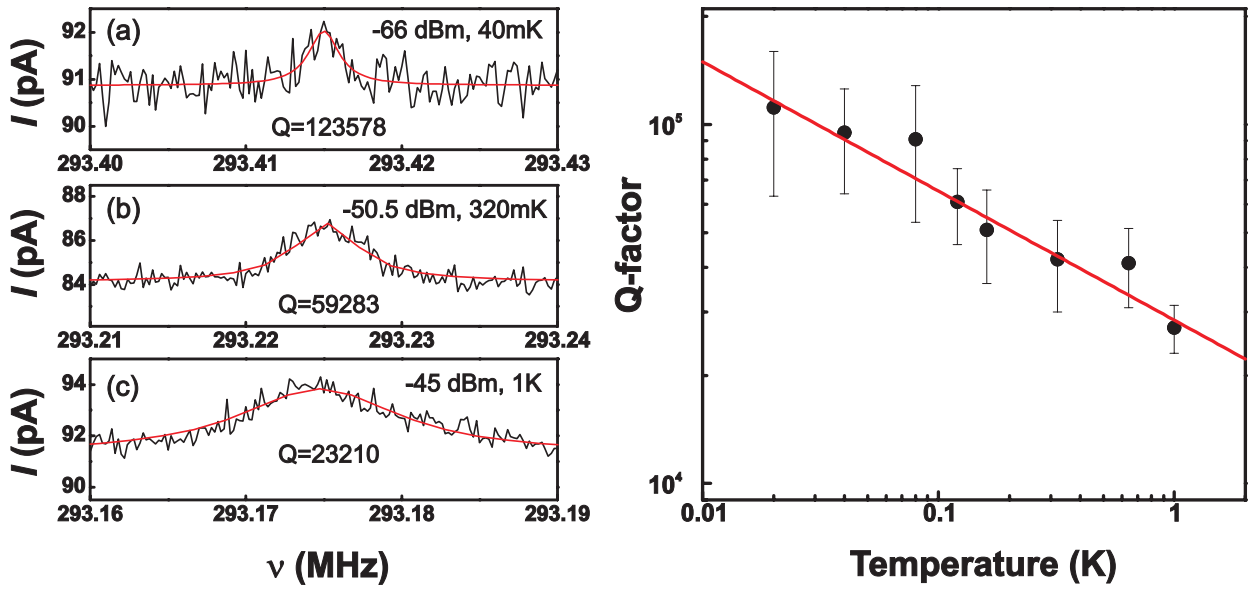


Figure 5: Temperature dependence of the Q-factor. (a-c) Fits of a squared harmonic oscillator response to the resonance in the linear regime at low powers for different temperatures at  $V_g = -5.16$  V and  $V_{sd} = 0.35$  mV. (d) A plot of the Q-factor vs. temperature obtained from linear response traces.  $Q$  decreases with increasing temperature. The red line shows a  $T^{-0.36}$  power law dependence (see text).